Synthesis, crystal structure and vibrational spectra characterization of MILa(PO3)4 (MI = Na, Ag)

Mohamed El Masloumi, Inhar Imaz, Jean-Pierre Chaminade, Jean-Jacques Videau, Michel Couzi, Mohamed Mesnaoui, Mohamed Maazaz

Synthesis, crystal structure and vibrational spectra characterization of $M^{I}La(PO_3)^4$ (M^{I} = Na, Ag)

Mohamed El Masloumia, Inhar Imaza, Jean-Pierre Chaminadea, Jean-Jacques Videau, Michel Couzi, Mohamed Mesnaoui, Mohamed Maazaz

Abstract : The single crystals of lanthanum metaphosphate MLa$(PO_3)_4$ (M=Na, Ag) have been synthesized and studied by a combination of X-ray crystal diffraction and vibrational spectroscopy. The sodium and silver compounds crystallize in the same monoclinic $P2_1/n$ space group (C_{2h}^5 factor group) with the following respective unit cell dimensions: a=7.255(2), b=13.186(3), $c = 10.076(2)$ Å, β=90.40(2)°, $V = 963.0(4)$ Å^3, Z=4 and a=7.300(5), b=13.211(9), $c = 10.079(7)$ Å, β=90.47(4)°, $V = 972.09(12)$ Å^3, Z=4. This three-dimensional framework is built of twisted zig-zag chains running along a direction and made up of PO_4 tetrahedra sharing two corners, connected to the LaO_8 and NaO_7 or AgO_7 polyhedra by common oxygen atoms to the chains. The infrared and Raman vibrational spectra have been investigated. A group factor analysis leads to the determination of internal modes of $(PO_3)^-$ anion in the phosphate chain.

1. Introduction

Research undertaken the latter years in our laboratory has shown the relationships between the structure and the luminescent properties of the silver ion in the condensed phosphates $Na_{1-x}Ag_x$ $M(PO_3)_3$ (M=Mg, Zn, Ba) [1] and [2] and in the diphosphates Na_{2-x} $Ag_xZnP_2O_7$ [3] and [4] where the two luminescent centres (single Ag^+ and Ag^+–Ag^+ pairs) have been correlated with the symmetry of the silver sites and with the ionocovalent character of the Ag^+–O bonds. In the same way, much works about other families of condensed phosphates with general formula $M^{I}M^{III}(PO_3)_4$ (where M^{I} is an alkali cation, Ag [5] and [6]) and M^{III} is a rare-earth trivalent cation [7], [8], [9] and [10], Bi [11] and [12] or Y [13] and [14] were published mainly for their optical properties. In particular, $LiNd(PO_3)_4$ [15] and [16] and $NaNd(PO_3)_4$ [17] have attractive performances as low threshold laser materials in agreement with the analysis of the crystal structures, respectively, by Hong [18] and Koizumi [19]. In addition, many of these compounds are isotropic and some of them are polymorphic. Moreover, these types of phosphates with cyclic or chain geometry are stable under normal conditions of temperature and moisture, and form all glasses after melting [20]. For example, Yb^{3+}–Er^{3+}-codoped $LiLa(PO_3)_4$ glass appears as a potential eye-safe laser material at 1535 nm [21].
In contrary, the literature gives few works and partial results on the crystallized and vitreous silver-earth rare metaphosphate. Only one complete work has been devoted to the $AgNd(PO_3)_4$ crystal structure [22]. The others references have only reported the Nd luminescent properties in $AgNd(PO_3)_4$ and in solid solutions $AgGd_{(1-x)}Nd_x(PO_3)_4$ [5] but no study is focused on the luminescent properties of Ag^+ cations or the optical interactions between silver and earth rare.
In this context, our research program consists to study the solid solution $Na_{(1-x)}Ag_xLa(PO_3)_4$ in crystallized and vitreous form in order to carry further the luminescent properties of silver ions. With this aim in view, it need to clarify the crystallographic structure of $NaLa(PO_3)_4$ and $AgLa(PO_3)_4$. Indeed, Ben Hassen et al. [23] proposed that $NaLa(PO_3)_4$ is an $NaNd(PO_3)_4$ isotype from powder crystallographic data which crystallizes in the monoclinic system $P2_1/c$ according to Ref. [17]. This structure attribution is in contradiction to Koizumi [19] that put forward a $P2_1/n$ space group and also to the expectations of Fedorova et al. [13]. In the same way, $AgLa(PO_3)_4$ [6] appears isotopic to $NaLa(PO_3)_4$ [23] with a $P2_1/c$ space group. Consequently, this paper is devoted to the synthesis and the crystal structure determination of the new form of $NaLa(PO_3)_4$ and $AgLa(PO_3)_4$ in order to try to remove this confusion. In addition, the nominal compounds have been characterized by micro-Raman and IR spectroscopy.

2. Experimental

2.1 Crystal growth :

Single crystals of $NaLa(PO_3)_4$ and $AgLa(PO_3)_4$ were prepared by a flux method following two different ways. At low temperature, the single crystals were similarly obtained from a previous process [9] using the reagents H_3PO_4 (85%), La_2O_3 (99.99%) and NaH_2PO_4 (99.99%) for $NaLa(PO_3)_4$ and the reagents H_3PO_4 (85%), La_2O_3 (99.99%), $AgNO_3$ (99.9+%) and $NH_4H_2PO_4$ (98%) for $AgLa(PO_3)_4$.
At high temperature the single crystals were obtained by spontaneous crystallization during slow cooling of a mixture containing excess of Na_2O and P_2O_5 versus the composition $NaLa(PO_3)_4$ in the ternary phase diagram $Na_2O–P_2O_5–La_2O_3$. The thermal cycle is the following: heating up to the complete melting of the mixture, then holding time at this temperature for 15 h, followed by a slow cooling (2–5 °C/h) to 750 °C and to room temperature (50 °C/h). Single crystals were separated by leaching the solidified melt with dilute hydrochloric acid (1 mol L^{-1}). In both cases crystals grew as elongated platelets with size up to 200×60×10 μm.

2.2 Structure refinement :

The single-crystal X-ray measurements were performed on a Nonius Kappa CCD diffractometer with a graphite monochromator using Mo*Kα* radiation. The chemical crystal data, the parameters used for the X-ray diffraction data collection and the results of crystal structure determinations of $NaLa(PO_3)_4$ and $AgLa(PO_3)_4$ are listed in Table 1. The empirical absorption corrections were carried out using SCALEPACK program [24]. Both structure were solved by direct methods and refined by full-matrix least-squares on F^2 values using SHELXL97 [25]. For Ag-containing compound the w*R* have a high value which can be explained by the rather bad quality of crystal (mosaicity is equal to 1.74). The final atomic coordinates with the equivalent isotropic displacement parameters together with the valence bond values based on bond strength analysis are reported in Table 2, in accordance with the formal oxidation states of La^{3+}, Na^{+}, Ag^{+}, P^{5+} and O^{2-} ions [26]. Selected interatomic distances are listed in Table 3. Further details of the crystal structure investigation(s) can be obtained from the Fachinformationszentrum Karlsruhe, 76344 Eggenstein-Leopoldshafen, Germany, (fax: (49) 7247 808 666; e-mail: crysdata@fiz.karlsruhe.de) on quoting the depository number CSD_415534 (For $AgLa(PO_3)_4$) and CSD_415535 (For $NaLa(PO_3)_4$).

2.3 Vibrational spectroscopy :

The infrared spectra of a mixture of KBr powder and powdered sample of $NaLa(PO_3)_4$ (3% weight) were recorded by the diffuse reflection technique using a Bruker IFS Equinox 55FTIR spectrometer (signal averaging 30 scans at a resolution of 4 cm^{-1}) in the range of 1500–400 cm^{-1}. The Raman spectrum of crystal sample was recorded with a Labram confocal micro-Raman instrument from Jobin–Yvon (typical resolution of 4 cm^{-1}), in backscattering geometry at room temperature. The system consists of a holographic notch filter for Rayleigh rejection, a microscope equipped with 10×, 50× and 100× objectives (the latter allowing a spatial resolution of less than 2 μm), and CCD detector. The source used for excitation was an Argon laser, with an output power of about 10 mW at 514.5 nm.

3 Results and discussion

3.1 Structure description

Projections on *ab* and *bc* planes are depicted in Fig. 1. The basic structure units of $Na(Ag)La(PO_3)_4$ are two meandering chains formed by corner-sharing PO_4 tetrahedra with the $(PO_3)^-$ formula. The chains $(PO_3)_n^-$ (two per unit cell) run along *a* direction. These chains are joined to one another by La and Na or Ag polyhedra forming a three-dimensional framework.

The lanthanum atom occupies one coordination polyhedron which can be described as a distorted Archimedian anti-prism (Fig. 2). The eightfold coordinated La atoms present regular La–O bond distances between 2.445 and 2.558 Å with a mean value of 2.51 Å for $NaLa(PO_3)_4$ and between 2.445 and 2.568 with a mean value of 2.52 Å for $AgLa(PO_3)_4$ (Table 3). Comparable values are encountered in other lanthanum oxide

structures [27]. Each La polyhedron is connected by means of common corners and by common faces with Na or Ag polyhedra.

The asymmetric unit contains four crystallographically independent $(PO_3)^-$ groups. All phosphate groups consist of a phosphorus atom coordinated to four oxygen atoms in a tetrahedron. Each P tetrahedron is connected by two common corners in *cis* position to other P tetrahedra (Fig. 1 and Fig. 3) giving rise to a twisted chain of general formula $(PO_3)_n^-$. The bond distances of P–O (non-bridging oxygen atom) vary from 1.477 to 1.494 Å for $NaLa(PO_3)_4$ and from 1.466 to 1.487 Å for $AgLa(PO_3)_4$. The P–O bond distances with bridging oxygen atoms along chains range from 1.581 to 1.595 Å and from 1.585 to 1.611 Å for sodium and silver crystals, respectively (Table 3). One can notice the orientation of the $(PO_3)^-$ tetrahedra chains which run all along a direction (Fig. 3).

There is only one monovalent cation type in the unit cell located on position 4*e*. Na or Ag atom is surrounded by seven oxygen atoms (Fig. 2). Their polyhedron is relatively irregular with five distances ranging from 2.399 to 2.583 Å (Na) and from 2.483 to 2.670 Å (Ag), one long distance, 2.749 Å (Na) and 2.820 Å (Ag) and one very long at 3.050 Å (Na) and 3.041 Å (Ag). Sodium or silver polyhedra are connected by common corners to $(PO_3)_n^-$ chains and by a common face to La dodecahedra. La–Na and La–Ag distances are, respectively, equal to 3.643 and 3.676 Å. The correspondence between expected and the experimental valence sum (see Table 2) confirm the sevenfold coordination of Ag and Na atoms.

Oxygen atoms can be divided in three groups depending on their cationic bonding. Oxygen atoms O(1), O(2), O(3), O(7), O(7), O(8) ,O(9), O(11) share Na or Ag atom, P and La atoms while O(3), O(4), O(10) and O(12) are only linked to P atoms. Oxygen atoms O(5), O(6), are only bounded to La and P atoms. Because of the highly covalent character of P–O bonds, the La–O bonds formed with oxygen of phosphate groups are weakened (Table 3).

3.2. Vibrational characterization of $NaLa(PO_3)_4$

$NaLa(PO_3)_4$ possesses a primitive unit with a monoclinic structure (space group $P2_1/n$) with four molecular units. The meandering metaphosphate chains consist of corner-sharing PO_4 groups and all atoms are located in general position on C_1 sites. The $NaLa(PO_3)_4$ cell contains therefore 18×4=72 atoms that give 72×3=216 vibrational modes in which are included three acoustic modes. Correlation of the symmetry species for C_1 sites to the C_{2h}^5 factor group leads to the irreducible representations of all the modes in $NaLa(PO_3)_4$ as follows:

$$\Gamma_{vib.NaLa(PO3)4}=54Ag+54Au+54Bg+54Bu.$$

The external modes include the optical translations (lattice vibrations) of four PO_4 ion groups and of two cations (Na^+ and La^{3+}) and the rotations (librations) of PO_4 tetrahedra. No rotational modes are possible with a monoatomic ion. The irreducible representations of optical translations, rotations and acoustic modes are, respectively:

- $\Gamma_{trans.}=18Ag+18Bg+17Au+16Bu$,
- $\Gamma_{rot.}=12Ag+12Bg+12Au+12Bu$,
- $\Gamma_{ac.}=1Au+2Bu$.

After subtraction, the irreducible representations corresponding to the internal modes of the metaphosphate chains are the following: $\Gamma_{int.}=24Ag$ (Ra)+24Bg (Ra)+24Au (IR)+24Bu (IR) which include:

- the PO_2 stretching modes: $\Gamma_{PO_2\ stret.}=8Ag$ (Ra)+8Bg (Ra)+8Au (IR)+8Bu (IR), including 16 antisymmetric vas PO_2 (8 Ra and 8 IR) modes and 16 symmetric vs PO_2 (8 Ra and 8 IR) modes,
- the POP stretching modes: $\Gamma_{POP\ stret.}=4Ag$ (Ra)+4Bg (Ra) +4Au (IR) +4Bu (IR) including 8 antisymmetric vas POP (4 Ra and 4 IR) modes and 8 symmetric vs POP (4 Ra and 4 IR) modes,

• the remaining internal modes, i.e. 12Ag(Ra)+12Bg(Ra)+12Au(IR)+12Bu(IR), correspond to the bending modes $\delta(PO_2)$ and δ(POP).

The IR and Raman spectra are, respectively, shown in Fig. 4 and Fig. 5. The frequencies of $(O_{1/2}\ PO_2O_{1/2})^-$ anion with $(PO_3)^-$ formula in chain metaphosphates are assigned on the basic of the $(PO_2)^-$ species and the P–O–P bridge. The band (IR) or line (Ra) number is in almost agreement with that of the theoretical prediction as shown in Table 4. The bands and lines observed in the regions 1000–1300 and 650–1000 cm^{-1} can be, respectively, attributed to the antisymmetric and the symmetric stretching vibrations (vas and vs) of $(PO_2)^-$ species and of POP bridges [28] and [29]. It is generally admitted that the symmetric stretching vibrations (vs POP) in chain metaphosphates occur in the range close to 700 cm^{-1} as strong Raman lines and weak infrared bands. The antisymmetric modes (vasPOP) are located around 900–800 cm^{-1} and give rise to strong infrared bands and weak Raman lines. In the low frequency region below 650 cm^{-1}, it is very difficult to distinguish the antisymmetric (δas) and symmetric (δs) bending modes of $(PO_2)^-$ species and δPOP bending. Moreover, these modes overlay with external modes.

A comparison of the Raman and infrared positions of bands shows that the majority of them are not coincident; this fact is in agreement with the centrosymmetric structure of $NaLa(PO_3)_4$.

4. Conclusion

Structure of the double phosphate of sodium or silver and lanthanum of formula $M^{I}La(PO_3)_4$ (M^{I}=Na, Ag) has been solved by a single crystal X-ray diffraction study. The sodium and silver compounds crystallize in the same monoclinic $P2_1/n$ space group (C_{2h}^5 factor group) and so definitively clarify the crystallographic structure of this double phosphate. The three-dimensional framework of $M^{I}La(PO_3)_4$ consists of twisted zig-zag chains of P tetrahedra running along *a* direction, with La and Na or Ag polyhedra connected by common corners to these chains and of coordination height and seven, respectively. They belong to a large family of isomorphous polyphosphates of general formula $NaM^{III}P_4O_{12}$, where *M*=Pr, Nd, Sm, Eu, Tb, Dy, Ho, Er, Tm, Y and Bi and Ag $M^{III}P_4O_{12}$ where *M*=La, Ce, Pr, Sm, Nd. The infrared and Raman vibrational study shows a good agreement between a group factor analysis results and the of the vibrational spectra assignment, i.e., 48 internal modes of $(PO_3)^-$ group, active in infrared and in Raman, for phosphate chains distributed among 16 PO_2 stretching modes, 8 POP stretching modes, and 24 $\delta(PO_2)$ and δ(POP) bending modes. The no coincidence of band position of infrared and Raman spectra confirms the centrosymmetric structure of these phases.

The luminescent property study of silver ions of the solid solution $Na_{(1-x)}Ag_xLa(PO_3)_4$ in crystallized and vitreous form is in progress and the one of Ln in glass and crystalline matrices $NaLn(PO_3)_4$ and $AgLn(PO_3)_4$ will be the subject of next papers.

Acknowledgments

This work was supported by the "Programme International de Coopération Scientifique du CNRS" (Contract No. 830). The authors wish to express grateful to P. Gravereau and V. Jubera for profitable discussions.

References

[1] I. Belharouak, H. Aouad, M. Mesnaoui, M. Maazaz, C. Parent, B. Tanguy, P. Gravereau and G. Le Flem, *J. Solid State Chem.* **145** (1999), pp. 97–103.

[2] H. Aouad, M. Maazaz and I. Belharouak, *Mater. Res. Bull.* **35** (2000), pp. 2457–2467.

[3] I. Belharouak, C. Parent, P. Gravereau, J.P. Chaminade, G. Le Flem and B. Moine, *J. Solid State Chem.* **145** (1999), pp. 97–103.

[4] I. Belharouak, P. Gravereau, C. Parent, J.P. Chaminade, E. Lebraud and G. Le Flem, *J. Solid State Chem.* **152** (2000), pp. 466–473.

[5] N.Y. Anisimova, N.N. Chudinova, E.V. Vasil'ev and A.A. Evdokimov, *Russ. J. Inorg. Chem.* **38** (1993) (7), pp. 1031–1034.

[6] D. Ben Hassen, N. Kbir-Ariguib and M. Trabelsi, *Thermochim. Acta* **65** (1983), pp. 35–42.

[7] I. Parreu, R. Sole, Jna Gavalda, J. Massons, F. Diaz and M. Aguilo, *Chem. Mater.* **17** (2005), pp. 822–828.

[8] I. Parreu, R. Sole, Jna Gavalda, J. Massons, F. Diaz and M. Aguilo, *Chem. Mater.* **15** (2003), pp. 5059–5064.

[9] W. Rekik, H. Naili and T. Mhiri, *Acta Crystallogr. C* **60** (2004), pp. 50–52.

[10] H. Ettis, H. Naili and T. Mhiri, *Cryst. Growth Design* **3** (2003) (4), pp. 599–602.

[11] K. Jaouadi, H. Naïli, N. Zouari, T. Mhiri and A. Daoud, *J. Alloys Comp.* **354** (2003), pp. 104–114.

[12] K. Jaouadi, N. Zouari, T. Mhiri and M. Pierrot, *J. Crystal Growth* **273** (2005), pp. 638–645.

[13] E.N. Fedorova, L.K. Shmatok, I.I. Kozhina and T.R. Barabanova, *Inorg. Mater. Engl. Trans.* **22** (1986), pp. 414–418.

[14] Y. Tsujimoto, Y. Fukuda and M. Fukai, *J. Electrochem. Soc.* **124** (1977) (4), pp. 553–556. [15] S.R. Chinn and H. Y-P. Hong, *Appl. Phys. Lett.* **26** (1975), pp. 646–651.

[16] K. Otsuka, J. Nakano and T. Yamada, *J. Appl. Phys.* **46** (1975), pp. 5297–5299.

[17] J. Nakano, K. Otsuka and T. Yamada, *J. Appl. Phys.* **47** (1976), pp. 2749–2750.

[18] H.Y.-P. Hong, *Mater. Res. Bull.* **10** (1975), pp. 635–640.

[19] H. Koizumi, *Acta Crystallogr. B* **32** (1976), pp. 2254–2256.

[20] A. Durif, *Crystal Chem. Condens. Phosphates* (1995), pp. 253–255.

[21] A.-F. Obaton, C. Parent, G. Le Flem, P. Thony, A. Brenier and G. Boulon, *J. Alloys Comp.* **300–301** (2000), pp. 123–130.

[22] V.K. Trunov, N.Yu. Anisimova, N.B. Karmanovskaya and N.N. Chudinova, *Izv. Akad. Nauk SSSR, Neoerg. Mat.* **26** (1990) (6), pp. 1288–1290.

[23] D. Ben Hassen, N. Kbir Arguib, M. Dabbabi and M. Trabelsi, *C. R. Acad. Sci. Paris* **294** (1982), pp. 375–378.

[24] Z. Otwinowski and W. Minor In: C.W. Carter and R.M. Sweet, Editors, *Methods in Enzymology, Macromolecular Crystallography* **vol. 276**, Academic Press, London (1997), pp. 307–326.

[25] G.M. Sheldrick, SHELXL97, A program for Crystal Structure refinement, University of Göttingen, Germany (1997).

[26] I.D. Brown and D. Altermatt, *Acta Crystallogr. B* **41** (1985), pp. 244–247.

[27] J.M. Cole, M.R. Lees, J.A.K. Howard, R.J. Newport, G.A. Saunders and E. Schoenherr, *J. Solid State Chem.* **150** (2000), pp. 377–382.

[28] A. Bertoluzza In: C. Sandorfy and T. Theophanides, Editors, *Spectroscopy of Biological Molecules*, D. Reidel Publishing Company, Dordrecht (1984), pp. 191–211.

[29] Meyer, H. Hobert, A. Barz and D. Stachel, *Vib. Spectrosc.* **6** (1994), pp. 323–332.

Table 1
Crystal data and structure refinement for $NaLa(PO_3)_4$ and $AgLa(PO_3)_4$

Crystal data		
Empirical formula	$NaLaP_4O_{12}$	$AgLaP_4O_{12}$
Crystal system	Monoclinic	Monoclinic
Space group	$P2_1/n$	$P2_1/n$
Z	4	4
Temperature (K)	293	293
Formula weight ($gmol^{-1}$)	477.78	562.66
Unit cell dimensions		
a(Å)	7.255(2)	7.300(5)
b(Å)	13.186(3)	13.211(9)
c(Å)	10.076(2)	10.079(7)
β (°)	90.40(2)	90.47(4)
Volume ($Å^3$)	963.0(4)	972.09(12)
D_X	3.295	3.845
$F(000)$	896	1040
Data collection		
Radiation	Mo$K\alpha$ ($\lambda = 0.71073$ Å)	Mo$K\alpha$ ($\lambda = 0.71073$ Å)
Monochromator	graphite	graphite
Diffractometer: Enraf-Nonius	Kappa CCD	Kappa CCD
Mosaicity (deg)	0.54	1.74
Absorption coefficient (mm^{-1})	5.211	7.073
θ range (deg)	2.55–26.37	2.54–26.36
Index ranges	$-9<h<9$	$-9<h<9$
	$-16<k<16$	$-16<k<16$
	$-12<l<12$	$-12<l<12$
Scan type	CCD scans	CCD scans
Reflections collected [$I>2\sigma(I)$]	7686	4956
Independent reflections [$I>2\sigma(I)$]	1753	1527
Refinement		
Refinement method	Full-matrix L.S. on F^2	Full-matrix L.S. on F^2
Parameters refined	164	164
Weighting scheme	$\omega = 1/[\sigma^2(F_o^2) + (\alpha P) + \beta P]$, where $P = (F_o^2 + 2F_c^2)/3$	$\omega = 1/[\sigma^2(F_o^2) + (\alpha P) + \beta P]$, where $P = (F_o^2 + 2F_c^2)/3$
Absorption correction		
α	0.042	0.074
β	0.508	2.971
Extinction coefficient	0.0057(3)	0.0056(7)
Goodness-of-fit	1.330	1.274
Final R indices [$I>2\sigma(I)$]		
R_1	0.020	0.055
wR_2	0.051	0.137
Maximum shift/esd	<0.0001	<0.0001
Largest diff. peak and hole ($eÅ^{-3}$)	1.32 (near La1); −0.4 (O9)	2.65, −1.96 (near La1)

Table 2
Atomic coordinates, equivalent isotropic displacement parameters (Å²), M^1 = Na (first line), *Ag (second line)* and bond valence analysis

Atom	Site	Site symmetry	*x*	*y*	*z*	$U_{(eq.)}$	Valence sum (Exp.)	Valence sum (Th.)
La1	4*e*	1	0.51371(3)	0.21650(2)	0.97570(2)	0.0078(1)	3.21	3
La1			*0.51324(9)*	*0.21545(5)*	*0.97618(7)*	*0.0173(2)*	*3.16*	*3*
Na1	4*e*	1	0.5002(3)	0.27953(16)	0.5678(2)	0.0236(7)	0.92	1
Ag1			*0.50133(15)*	*0.27684(8)*	*0.56809(12)*	*0.0331(4)*	*0.87*	*1*
P1	4*e*	1	0.27150(16)	0.08863(9)	0.69395(12)	0.0087(3)	5.00	5
			0.2668(4)	*0.0880(2)*	*0.6960(3)*	*0.0175(9)*	*5.02*	*5*
P2	4*e*	1	0.35709(16)	−0.12724(9)	0.69277(11)	0.0079(3)	4.97	5
			0.3557(4)	*−0.1265(2)*	*0.6931(3)*	*0.0175(9)*	*5.08*	*5*
P3	4*e*	1	0.75186(16)	−0.09818(9)	0.75661(12)	0.0079(3)	4.99	5
			0.7472(4)	*−0.0973(2)*	*0.7537(3)*	*0.0171(9)*	*5.09*	*5*
P4	4*e*	1	0.88372(16)	0.11438(9)	0.76447(12)	0.0082(3)	5.04	5
			0.8809(4)	*0.1138(2)*	*0.7626(3)*	*0.0168(9)*	*5.03*	*5*
O1	4*e*	1	0.2418(4)	0.1587(2)	0.5808(3)	0.0131(10)	1.96	2
			0.2353(11)	*0.1569(6)*	*0.5824(9)*	*0.023(3)*	*1.95*	*2*
O2	4*e*	1	0.4303(4)	0.1084(3)	0.7838(3)	0.0166(10)	1.88	2
			0.4225(11)	*0.1069(6)*	*0.7858(9)*	*0.021(3)*	*1.92*	*2*
O3	4*e*	1	0.0933(4)	0.0795(3)	0.7849(3)	0.0129(10)	2.11	2
			0.0879(11)	*0.0785(6)*	*0.7847(8)*	*0.019(3)*	*2.12*	*2*
O4	4*e*	1	0.2849(4)	−0.0225(2)	0.6316(3)	0.0114(9)	2.11	2
			0.2814(11)	*−0.0233(6)*	*0.6316(8)*	*0.017(2)*	*2.09*	*2*
O5	4*e*	1	0.2909(5)	−0.2091(2)	0.6029(3)	0.0122(10)	1.80	2
			0.2870(11)	*−0.2087(6)*	*0.6053(9)*	*0.021(3)*	*1.95*	*2*
O6	4*e*	1	0.3166(5)	−0.1331(2)	0.8369(3)	0.0123(10)	1.92	2
			0.3205(12)	*−0.1317(6)*	*0.8359(9)*	*0.023(3)*	*1.98*	*2*
O7	4*e*	1	0.5742(4)	−0.1207(2)	0.6689(3)	0.0109(9)	2.15	2
			0.5689(11)	*−0.1201(6)*	*0.6659(8)*	*0.019(3)*	*2.15*	*2*
O8	4*e*	1	0.7156(5)	−0.1045(2)	0.9024(3)	0.0127(10)	1.87	2
			0.7092(12)	*−0.1023(6)*	*0.8967(9)*	*0.023(3)*	*1.95*	*2*
O9	4*e*	1	0.9045(4)	−0.1630(3)	0.7072(3)	0.0132(10)	1.99	2
			0.8972(12)	*−0.1619(6)*	*0.7046(9)*	*0.023(3)*	*1.99*	*2*
O10	4*e*	1	0.7883(5)	0.0146(2)	0.7103(3)	0.0129(9)	2.20	2
			0.7864(12)	*0.0149(6)*	*0.7051(9)*	*0.021(3)*	*2.17*	*2*
O11	4*e*	1	0.8684(4)	0.1897(3)	0.6564(3)	0.0130(10)	2.02	2
			0.8687(12)	*0.1900(6)*	*0.6556(9)*	*0.022(3)*	*1.98*	*2*
O12	4*e*	1	0.8147(4)	0.1431(3)	0.8977(3)	0.0127(9)	2.02	2
			0.8084(12)	*0.1402(6)*	*0.8956(9)*	*0.022(3)*	*2.00*	*2*

Table 3
Selected lengths (Å) in $M^{I}La(PO_3)_4$ (M^{I} = Na, Ag)

$NaLa(PO_3)_4$		$AgLa(PO_3)_4$	
La–O		*La–O*	
La1–O2	2.473(3)	La1–O2	2.481(9)
La1–O12	2.519(3)	La1–O12	2.514(9)
La1–O5_*c*	2.539(3)	La1–O5_*c*	2.540(8)
La1–O9_*e*	2.506(3)	La1–O9_*e*	2.528(9)
La1–O6_*g*	2.500(3)	La1–O6_*g*	2.500(9)
La1–O8_*g*	2.546(3)	La1–O8_*g*	2.559(9)
La1–O11_*i*	2.445(3)	La1–O11_*i*	2.445(9)
La1–O1_*k*	2.558(3)	La1–O1_*k*	2.567(8)
Na–O		*Ag–O*	
Na1–O1	2.464(4)	Ag1–O1	2.512(8)
Na1–O12_*h*	2.398(4)	Ag1–O12_*h*	2.483(9)
Na1–O5_*f*	2.479(4)	Ag1–O8_*e*	2.670(9)
Na1–O9_*e*	2.482(4)	Ag1–O9_*e*	2.535(9)
Na1–O8_*e*	2.583(4)	Ag1–O5_*f*	2.509(9)
Na1–O6_*c*	2.749(4)	Ag1–O6_*c*	2.820(9)
Na1–O11	3.050(4)	Ag1–O11	3.041(9)
P–O		*P–O*	
P1–O1	1.481(3)	P1–O1	1.479(9)
P1–O2	1.483(3)	P1–O2	1.469(9)
P1–O3	1.594(3)	P1–O3	1.594(9)
P1–O4	1.597(3)	P1–O4	1.611(8)
P2–O4	1.599(3)	P2–O4	1.591(8)
P2–O5	1.486(3)	P2–O5	1.486(9)
P2–O6	1.484(3)	P2–O6	1.466(10)
P2–O7	1.597(3)	P2–O7	1.585(9)
P3–O7	1.585(3)	P3–O7	1.597(9)
P3–O8	1.495(3)	P3–O8	1.472(10)
P3–O9	1.487(4)	P3–O9	1.477(9)
P3–O10	1.581(3)	P3–O10	1.588(9)
P4–O10	1.582(3)	P4–O10	1.585(9)
P4–O11	1.477(4)	P4–O11	1.478(9)
P4–O12	1.484(3)	P4–O12	1.487(9)
P4–O3_*a*	1.600(3)	P4–O3_*a*	1.595(9)
Na–Na		*Ag–Ag*	
Na1–Na1	5.972(3)	Ag1–Ag1	6.054(2)
La–La		*La–La*	
La1–La1_*g*	5.743(1)	La1–La1_*g*	5.716(1)
Na–La		*Ag–La*	
Na1–La1_*m*	3.643(3)	Ag1–La1_*m*	3.676(1)

$a = 1+x, y, z$; $b = 1/2-x, -1/2+y, 3/2-z$; $c = 1/2-x, 1/2+y, 3/2-z$; $d = 3/2-x, -1/2+y, 3/2-z$; $e = 3/2-x, 1/2+y, 3/2-z$; $g = 1-x, -y, 2-z$; $h = -1/2+x, 1/2-y, -1/2+z$; $i = -1/2+x, 1/2-y, 1/2+z$; $j = 1/2+x, 1/2-y, -1/2+z$; $k = 1/2+x, 1/2-y, 1/2+z$.

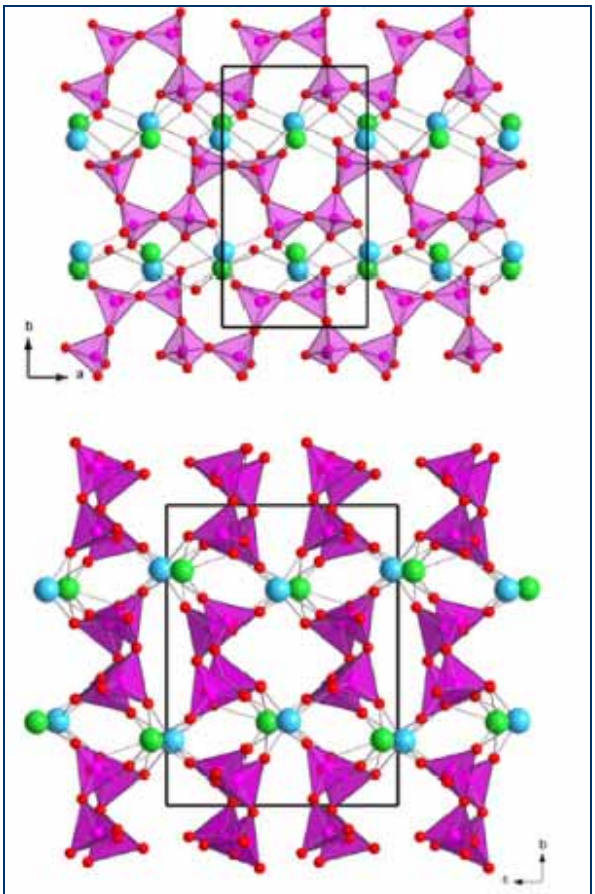

Fig. 1. Projection in *ab* and *bc* planes of the $M^1La(PO_3)_4$ structure (M^1 = Na, Ag); Na and La atoms are, respectively, presented by green and blue spheres).

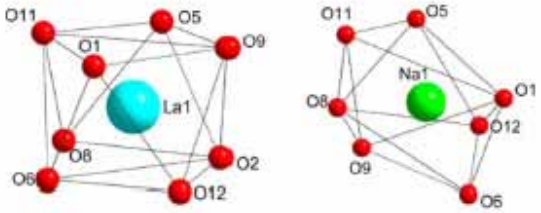

Fig. 2. Coordination polyhedron of Na or Ag and La in $M^1La(PO_3)_4$ (M^1 = Na, Ag).

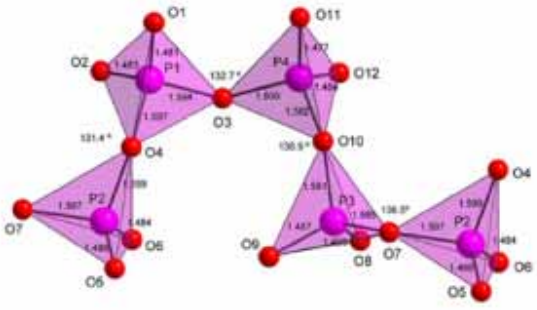

Fig. 3. Connexion of the phosphate units in $(PO_3)^-_n$ chain; the distances are given in Å and the angles in degree.

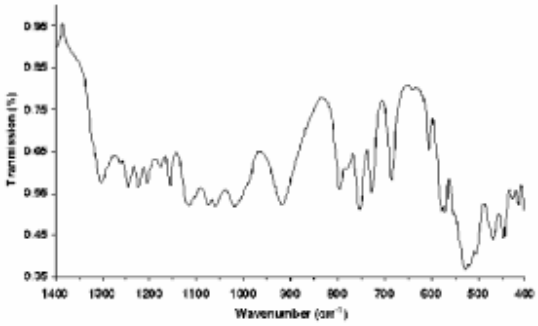

Fig. 4. FT-IR spectrum of $NaLa(PO_3)_4$.

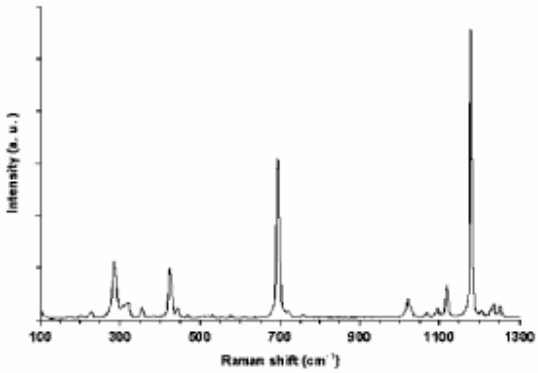

Fig. 5. Raman spectrum of $NaLa(PO_3)_4$.

Table 4
Band assignment (cm^{-1}) for $NaLa(PO_3)_4$

IR	Raman	Assignment
1300s		$\nu_{as}PO_2 + \nu_sPO_2$
1255w	1251vw	
1244m	1234vw	
1210m	1229w	
1203m	1204w	
1175w	1179vs	
1175s	1155vw	
1124s	1124vw	
	1120m	
1113s	1101vw	
1099s	1094w	
1070s	1071vw	
1055s	1067w	
1051s	1047vw	
	1041vw	
1030w	1025w	
1013s	1021w	
1005w		
987m	970vw	$\nu_{as}POP + \nu_sPOP$
914vs	908vw	
	847vw	
	808vw	
	805vw	
792s		
772m		
750vs	759w	
725s	721w	
	700s	
685m		
667vw		
	612w	$\delta PO_2 + \delta POP$ + external modes
637vw	578w	
606m		
577vs	555vw	
571vs	558vw	
548s	530v	
	516w	
525vs	510w	
517vs	469vw	
503s	457vw	
467s	444w	
446s	424m	
426m		
415m	406vw	
	382vw	
	365vw	
	355w	
	319vw	
	307w	
	296m	
	247vw	
	227w	
	203vw	
	178vw	
	174w	
	168vw	
	160vw	
	139vw	
	110vw	

Note: vs: very strong, s: strong, m: medium, w: weak, vw: very weak.